Characterization of ^{7}Li$(p,n)^7$Be neutron yields from laser produced ion beams for fast neutron radiography

K. L. Lancaster,[1,2] S. Karsch,[1] H. Habara,[1] F. N. Beg,[2] E. L. Clark,[2] R. Freeman,[3] M. H. Key,[4] J. A. King,[3,4] R. Kodama,[5] K. Krushelnick,[2] K. W. D. Ledingham,[6] P. McKenna,[6] C. D. Murphy,[1,2] P. A. Norreys,[1] R. Stephens,[7] C. Stöeckl,[8] Y. Toyama,[5] M. S. Wei,[2] and M. Zepf[9]
[1]*CCLRC Rutherford Appleton Laboratory, Chilton, Oxon OX11 0QX, United Kingdom*
[2]*The Blackett Laboratory, Imperial College, London SW7 2BZ, United Kingdom*
[3]*Department of Applied Science, University of California, Davis, 1 Shields Ave., Davis, California*
[4]*Lawrence Livermore National Laboratory, Livermore, California 94550*
[5]*Institute of Laser Engineering, Osaka University, 2-6 Yamada-oka, Suita, Osaka T565, Japan*
[6]*Department of Physics, University of Strathclyde, Glasgow G4 0NG, United Kingdom*
[7]*General Atomics, P.O. Box 85608, San Diego, California 92186-5608*
[8]*Laboratory of Laser Energetics, University of Rochester, Rochester, 250 E. River Road, New York 14623-1299*
[9]*Queens university of Belfast, Belfast BT7 1NN, United Kingdom*

(Received 7 November 2003; accepted 7 April 2004; published online 27 May 2004)

Investigations of ^{7}Li$(p,n)^7$Be reactions using Cu and CH primary and LiF secondary targets were performed using the VULCAN laser [C.N. Danson *et al.*, J. Mod. Opt. **45**, 1653 (1997)] with intensities up to 3×10^{19} W cm^{-2}. The neutron yield was measured using CR-39 plastic track detector and the yield was up to 3×10^8 sr^{-1} for CH primary targets and up to 2×10^8 sr^{-1} for Cu primary targets. The angular distribution of neutrons was measured at various angles and revealed a relatively anisotropic neutron distribution over 180° that was greater than the error of measurement. It may be possible to exploit such reactions on high repetition, table-top lasers for neutron radiography. © *2004 American Institute of Physics.* [DOI: 10.1063/1.1756911]

I. INTRODUCTION

There has been considerable research into energetic proton and ion beams produced in short pulse, high intensity, laser–plasma interactions.[1–9] The protons appear to be accelerated from two regions of the target. At the front of the target, ion acceleration can occur by a number of mechanisms: electrostatic sheath expansion into the vacuum,[10] a Coulomb explosion of a channel formed in the preformed plasma generated by the pedestal of the laser pulse,[11] hole-boring induced by charge separation,[12] and by electrostatic shocks.[13] At the rear surface of the target, an electrostatic sheath, generated by fast electrons that reach there but cannot escape the target due to space charge build up, also accelerates ions.[14]

These laser produced proton beams can be used to induce reactions in secondary cold targets to produce a bright source of neutrons. Neutrons from laser–plasma interactions could be developed as a source for fast neutron radiography.[15] Neutrons provide a good method of differentiating between high and low Z materials due to the fact that they are attenuated by atomic nuclei. Low Z ions scatter neutrons more effectively than high Z ions. X rays, by contrast, are attenuated by electrons and are less able to distinguish between nuclei with different atomic mass. Both thermal and fast neutrons can be used for imaging purposes, but fast neutrons are ideal for imaging the interior of dense objects that would attenuate thermal neutrons.

Laser produced protons can also be used for imaging purposes.[16–21] Protons can be attenuated by both collisional processes and by electromagnetic fields. They can image high and low Z materials as well as provide information on static and transient electromagnetic fields that are generated in laser–plasma interactions. Much development has been done to characterize the source[19–21] and the technique has been used to image transient effects[17,18] and static objects.[16,19] However the advantage of developing neutron radiography is that it can potentially be used to image large, bulky objects and will be unaffected by electromagnetic fields.

There are several methods of fast neutron radiography. The first one relies on time-of-flight detection of gamma rays emitted from nuclei excited by the neutron beam along with neutron transmission measurement to gain a spatially resolved picture of elemental composition with position.[22] This method has been proposed for the detection of hidden drugs and buried layers of different elemental composition. Second it is possible to employ neutron resonance radiography[23] to determine elemental composition. By varying the energy of the neutron beam, resonances in the cross section of neutrons incident on particular nuclei can be utilized. Neutron scattering is maximized at these resonances and leads to a reduction in neutron transmission. By spatially resolving the neutron flux an image of the element's line density can be obtained. Even the nonresonant scattering depends on material density fluctuations and can be used in a similar way to obtain an image.[24]

We present here the first study of (p,n) reactions induced in secondary LiF targets from laser-produced proton beams that reveals both high neutron fluxes—up to 3

$\times 10^8$ sr^{-1}—and an anisotropy in the angular distribution of neutrons. Similar measurements were made by Disdier *et al.*[25] using the D$(d,n)^3$He reaction. The VULCAN laser facility[26] provided 1 ps, 1.053 μm pulse with a rectangular near-field beam profile (200 mm$\times$110 mm). The full aperture beam was focused on target using f/4.5 and f/3.5 off-axis parabolas at both normal and 45° incidence to the target normal, respectively. In these experiments, the laser was focused to a 10 μm focal spot. The energy contained within that spot was ~30% of the total incident energy (up to 80 J) according to an equivalent plane monitor, giving focused intensities up to 3×10^{19} W cm^{-2}.

II. EXPERIMENTAL METHOD

Thin foil targets of Mylar (50 mm) and copper (25 mm) were used to produce a proton beam with equivalence to Refs. 1–7. A secondary LiF catcher target (3.4 mm thick) was used to generate neutrons via the ^{7}Li$(p,n)^7$Be reaction. The primary and secondary targets were separated by a distance of 0.5 cm. The proton beam was diagnosed by using 25 μm Cu targets without a LiF catcher present. The proton beam diagnostic consisted of a stack of alternating layers of CR-39 plastic nuclear track detector, of dimensions 5 cm $\times$5 cm$\times$1 mm, and radiochromic film (RCF) of dimensions 5 cm$\times$5 cm$\times$110 μm. CR-39 is a polymer developed specially to detect charged particles. Charged particles incident on the detector cause damage to the polymer chains which can be etched away to reveal particle tracks (more details in following paragraphs). Radiochromic film consists of a transparent nylon film, ~110 μm thick coated with an organic dye that changes from transparent to deep blue when exposed to ionizing radiation. Both CR-39 and RCF provide spatial and spectral information, although RCF is sensitive to electrons. The first layer of the stack was a 12 μm Al filter permitting protons of $E>1$ MeV. The second layer was RCF permitting protons of $E>3$ MeV, the third layer was CR-39. RCF and CR-39 were placed in alternating layers up to a total thickness of ~2 cm.

Several methods of neutron detection were employed to obtain a picture of the angular distribution of the neutrons. Current mode time-of-flight (TOF) detectors consisting of plastic scintillators, which detect neutrons via elastic scattering off protons in the scintillator, coupled to photomultiplier tubes were used to diagnose the energy of the neutrons. Time-of-flight signals were recorded on an oscilloscope.

Plastic nuclear track detectors (CR-39), shielded with 2 mm of lead front and back, were also used to measure neutron yield via damage caused by knock-on protons. After exposure, the detectors are etched in concentrated sodium hydroxide solution at 80 °C for 3 hours. Knock-on protons propagate in the track detector and damage the polymer bonds via ionization. After etching the damage tracks are revealed as pits in the surface of the detector. Typical proton tracks have a diameter ~10 μm. By counting the total number of pits and correcting for the solid angle and sensitivity, it is possible to infer a neutron yield. The sensitivity of knock-on protons in CR-39 detectors to neutrons with energies of 2.5 MeV is 1.0×10^{-4}.[27] As our peak neutron energies are near this value it is reasonable to assume this sensitivity.

In this paper, all angles are defined with respect to the target normal from the rear surface as depicted in Fig. 1. In the first neutron production experiment, mylar primary and LiF secondary targets were used. An f/3.5 off-axis parabola focused a 1 ps, 1.053 μm pulse onto target at 135°. CR-39 was placed in at 0° and at 180° to obtain the yield in these directions. A time-of-flight detector was placed 2.32 m away at an angle of 88°. In the second experiment, copper primary and LiF secondary targets were used. An f/4.5 off-axis parabola focused a 1 ps, 1.053 μm pulse at normal incidence to the target. CR-39 was placed close to the target (7–10 cm) at 0°, 60°, 110°, and 160° to obtain the angular distribution of neutrons. The current mode TOF detector was placed 2.25 m away at an angle of 70°.

III. RESULTS AND DISCUSSION

The proton beam produced from Cu targets was characterized using a CR-39 stack. The stack revealed a cutoff in the energy of the protons of 15 MeV. Figures 2(a) and 2(b) show CR-39 images of the proton beam. Protons were observed on these slides on the front and back surfaces but not on the third layer. From well-known stopping characteristics of protons in RCF/CR-39 it is possible to calculate the proton energies. The front side of slide (a) corresponds to protons of 3 MeV and the back side corresponds to 10 MeV. The front side of slide (b) corresponds to protons of 11 MeV and the back side, 15 MeV.

Figure 3(a) shows a typical time-of-flight measurement obtained using the copper primary targets. The neutron energy peaks at ~2.1 MeV. Figure 3(b) shows a typical time-of-flight spectrum with CH primary targets. The neutron energy peaks at ~1.8 MeV. The gamma ray yield is higher from the Cu primary target because the bremsstrahlung yield is proportional to Z.

The black squares in Fig. 4 represent measurements of the angular distribution of neutrons at various angles for an energy on target of 69 J and an intensity of 2.5×10^{19} W cm^{-2}. The target consisted of 50 μm thick Mylar plastic. The peak yield was found to be up to 2×10^8 sr^{-1} at 0° and 3×10^8 sr^{-1} at 180°. The triangles, circles, and squares in Fig. 4 represent measurements of the angular distribution of neutrons using the Cu primary targets. The peak yield was up to 1.5×10^8 sr^{-1} at 0° and 2×10^8 sr^{-1} at 160/170°.

There is a difference of a factor of 2 in the neutron yield between using copper targets and plastic targets. This difference could be due to a number of factors. The angle of incidence for CH primaries was 45° and for Cu primaries, normal. Since the angle of incidence of p-polarized light was 45° for CH the absorption of laser energy may have been enhanced due to resonant absorption and thus more protons were accelerated. One may also consider that the laser energy may have been sufficient to deplete the entire hydrogen contamination layer from the Cu. Once the hydrogen contamination layer had been depleted from the plastic target

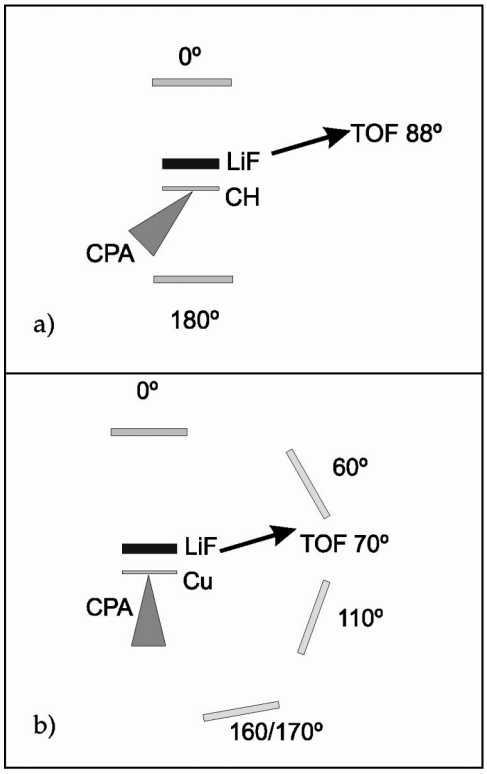

FIG. 1. (a) Experimental setup with CH primary target, (b) experimental setup with Cu primary target.

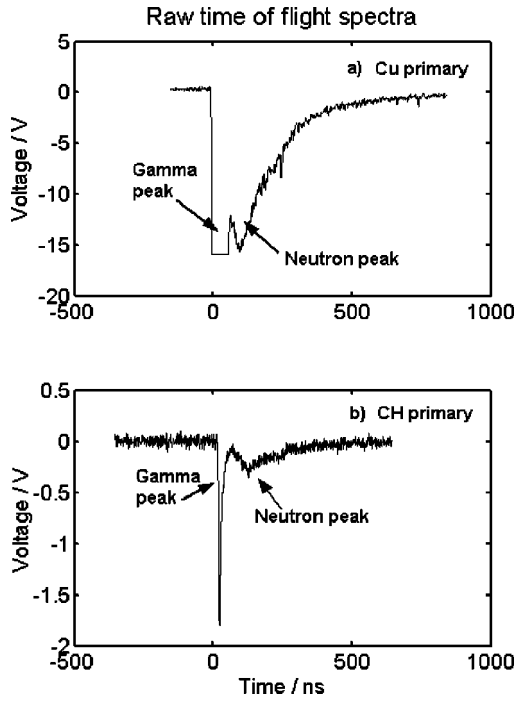

FIG. 3. Two raw time of flight spectra, (a) neutron spectrum produced from using Cu primary targets, and (b) neutron spectrum produced from using CH primary targets.

there may have been sufficient energy to liberate protons from hydrogen deeper into the surface layers of the plastic hence producing more protons. This effect is similar to that observed by Snavely *et al.*[2] where they observed ~ 5 times more protons from CH targets than Au targets. Although these are possibilities, a factor of 2 difference is considered typical of shot-to-shot fluctuations[28] and therefore cannot reliably be counted as significant.

From the IAEA Drosg-2000 code the cross section for the $^{7}\mathrm{Li}(p,n)$ reaction shows the neutron yield at 0° should be a factor of 3 greater than at 180°. The solid line in Fig. 4 represents this distribution and was generated for this paper using the Monte Carlo code described in Ref. 29. The code is a 3D, Monte Carlo method that tracks ions within various target and catcher geometries. Ion energy loss and stopping is calculated by a modified Bethe–Bloch equation for cold matter and plasma. Reaction cross sections are taken from the Drosg-2000 tables. Neutron scattering is modeled using outputs from a Monte Carlo code, MCNP, developed by Los Alamos National Laboratory.[30]

The yields on this line are arbitrary but it shows the relative distribution at each angle. The measured and simulated distributions match well in the forward hemisphere but there is a discrepancy in the backward direction. Other reactions must be contributing to the final yield here. Higher order Li reactions are insignificant here as their cross section is small, but the measured difference between 0° and 180° in this paper is $1\times10^{8}n$ sr^{-1}. Therefore, other reactions must be considered.

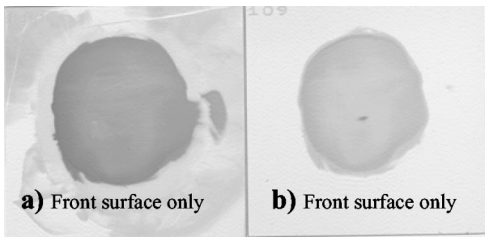

FIG. 2. Front side of CR-39 used to diagnose proton beam. Front of (a) corresponds to protons of 3 MeV and the back side corresponds to 10 MeV. Front of (b) corresponds to protons of 11 MeV and the back side, 15 MeV. The figure only depicts the front sides of both CR-39 slides.

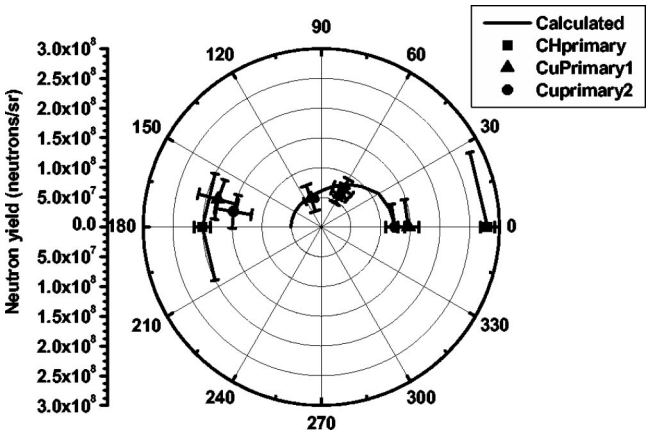

FIG. 4. Measured and simulated neutron angular distributions. Solid line represents the simulated distribution, the squares represent measurements using CH primary targets, and the circles and triangles represent measurements using Cu primary targets.

The CR-39 was shielded with lead and so the ^{208}Pb$(p,n)^{208}$Bi reaction may be significant for the 180° blow-off direction where energetic protons were incident directly onto the Pb material. In the other directions, this reaction is not considered important—in the forward direction, the protons are stopped in the LiF target, and at oblique angles the detectors are well outside the measured cone angle of the proton beams. The cross section for this reaction is ~6.56 barn at 25 MeV. The yield of protons produced at 180° can be greater than that at 0° and will be at a minimum at 90°. At 0° all protons should be stopped in the LiF tablet and so the Li(p,n) neutrons will make up a significant part of the yield here. However at 180° there may be a significant contribution from the ^{208}Pb$(p,n)^{208}$Bi reaction. To obtain a more qualitative estimate of the importance of the ^{208}Pb$(p,n)^{208}$Bi reaction the same Monte Carlo code was used to estimate of the yield of neutrons produced by this reaction. The fast rise in the ^{208}Pb$(p,n)^{208}$Bi cross section with energy (Fig. 5) above 10 MeV causes a strong dependence of the neutron yield from this reaction on the hot part of the proton spectrum. To model this we assumed protons in an exponential spectrum of temperature 8 MeV and a 40° divergence hitting either the LiF tablet or the lead shielding of the detector at 180°. We varied the cutoff of the proton spectrum from 5 to 30 MeV and plotted the neutrons entering the detector at 180° from both reactions. Because of the geometry of the experiment nearly half of the neutrons generated in the lead enter the CR-39 and they constitute a significant amount of the total measured neutrons for cutoff energies greater than 15 MeV. Although the proton spectrum in the blow off direction was not measured in this experiment it was determined in a previous experiment to extend between 15 and 25 MeV. This makes the assumption of the lead causing the high yield at 180° very likely. Note that all the other positions of CR-39 are either obstructed by the LiF tablet or are outside the blow off direction so that the lead reaction is strongly suppressed here.

IV. ERROR ANALYSIS

To assist in the error analysis, a test slide of CR-39 was etched along side the exposed slides to obtain a measurement of background levels. This slide was analyzed in exactly the same way at the exposed slides and a background count was obtained.

The spread on the number of positive counts on each slide, $\sqrt{n}$, was summed in quadrature with the background error to obtain a value for the absolute error of each measurement. The error bars on the polar plot in Fig. 3 represent these errors. The error on the angle measurement arises from the fact that the detector has a finite size and so will cover a small range of angles.

V. PRACTICAL IMPLICATIONS FOR NEUTRON RADIOGRAPHY

To be useful for radiographic applications a yield of $\sim 10^{11-13}$ neutrons sr^{-1} is required. To produce this yield of neutrons the laser must deliver more energy. From simple scaling of current experiments it is possible to infer the laser energy needed to produce such yields. The neutron yield, $Y_n \propto \sigma E \eta$ where σ is the cross section, E is the laser energy on target, and η is the conversion efficiency of laser energy to protons. The conversion efficiency of laser energy to protons has been seen to increase with increasing laser energy. Measurements on the VULCAN system show a conversion efficiency of between 0.1% and 5%.[31] At energies >400 J it has been shown that the conversion efficiency increases to 12%.[2] However, with higher energy lasers the protons will be more energetic and the average proton energy will increase. The giant resonance in the cross section of the ^{7}Li$(p,n)^{7}$Be reaction spans an incident proton energy range of 3–7 MeV up to a value of 320 mb and so for higher energies a different reaction should be utilized. It is preferable to utilize an element that has a peak in the (p,n) cross section for higher energy protons such as the lead reaction that we have discussed in this paper, ^{208}Pb$(p,n)^{208}$Bi. This reaction has a cross section of ~6 barns for 15–25 MeV incident proton energy. The proton range will increase with proton energy so the thickness of the target should be increased.

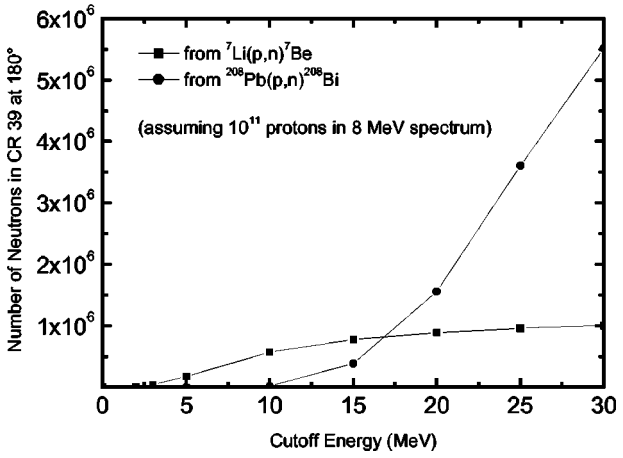

FIG. 5. Monte Carlo generated neutron numbers with incident proton cutoff energy for ^{208}Pb$(p,n)^{208}$Bi (circles) and ^{7}Li$(p,n)^{7}$Be (squares).

To exploit neutron radiography in the current scheme it is planned to conduct experiments in which laser produced neutrons pass through a test object and are attenuated according to the materials present. A neutron imaging plate or a standard image plate such as BAS–TR coupled with a polyethylene converter can be used to detect the neutrons.[32] It may also be possible to activate a sample with the neutrons and then place this on to a standard image plate to obtain an image.

VI. CONCLUSIONS

We have presented neutron yields from ^{7}Li(p,n) reactions using laser-generated proton beams from Cu and CH primary foils incident on a LiF secondary target. The CH foil produced neutron yields of up to 3×10^{8} neutrons/steradian for p-polarized irradiation and the Cu foils produced neutron yields of up to 2×10^{8} neutrons/steradian for normal incidence irradiation. The yields for all foil types were slightly higher at 180° compared to 0°. This may be attributed to the ^{208}Pb$(p,n)^{208}$Bi reaction in the lead shielding on the CR-39.

This reaction should not be significant at 0° as all the protons are stopped in the LiF tablet. Between 0° and 60/110° the distribution agrees well with the calculated distribution and it is therefore probable that the yields here are due to reactions in the LiF tablet.

ACKNOWLEDGMENTS

We thank all the staff of the Central Laser Facility for their help in the execution of this work.

This work was supported by a joint United Kingdom Engineering and Physical Sciences Research Council/ Ministry of Defense Grant No. GR/R16778. American colleagues acknowledge support from the U.S. Department of Energy Contract No. W-7405-Eng-48. Japanese colleagues acknowledge the Japan Society for the Promotion of Science.

[1] E. L. Clark, K. Krushelnick, J. R. Davies, M. Zepf, M. Tatarakis, F. N. Beg, A. Machacek, P. A. Norreys, M. I. K. Santala, I. Watts, and A. E. Dangor, Phys. Rev. Lett. **84**, 670 (2000).
[2] R. A. Snavely, M. H. Key, S. P. Hatchett, T. E. Cowan, M. Roth, T. W. Phillips, M. A. Stoyer, E. A. Henry, T. C. Sangster, M. S. Singh, S. C. Wilks, A. MacKinnon, A. Offenberger, D. M. Pennington, K. Yasuike, A. B. Langdon, B. F. Lasinski, J. Johnson, M. D. Perry, and E. M. Campbell, Phys. Rev. Lett. **85**, 2945 (2000).
[3] M. Zepf, E. L. Clark, F. N. Beg, R. J. Clarke, A. E. Dangor, A. Gopal, K. Krushelnick, P. A. Norreys, M. Tatarakis, U. Wagner, and M. S. Wei, Phys. Rev. Lett. **90**, 064801 (2003).
[4] K. Krushelnick, E. L. Clark, M. Zepf, J. R. Davies, F. N. Beg, A. Machacek, M. I. K. Santala, M. Tatarakis, I. Watts, P. A. Norreys, and A. E. Dangor, Phys. Plasmas **7**, 2055 (2000).
[5] A. Mackinnon, M. Borghesi, S. P. Hatchett, M. H. Key, P. K. Patel, H. Campbell, A. Schiavi, R. Snavely, S. C. Wilks, and O. Willi, Phys. Rev. Lett. **86**, 1769 (2001).
[6] M. Roth, H. Blazevic, M. Geissel, T. Schlegel, T. E. Cowan, M. Allen, J. C. Gauthier, P. Audebert, J. Fuchs, J. Meyer-ter-Vehn, M. Hegelich, and S. Karsch, Phys. Rev. ST Accel. Beams **5**, 061301 (2002).
[7] A. Maksimchuck, S. Gu, K. Flippo, D. Umstadter, and V. Buchenkov, Phys. Rev. Lett. **84**, 4108 (2000).
[8] M. Hegelich, S. Karsch, G. Pretzler, D. Habs, K. Witte, W. Guenther, M. Allen, A. Blazevic, J. Fuchs, J. C. Gauthier, M. Geissel, P. Audebert, T. Cowan, and M. Roth, Phys. Rev. Lett. **89**, 085002 (2002).
[9] K. W. D. Ledingham, P. McKenna, and R. P. Singhal, Science **300**, 1107 (2003).
[10] S. J. Gitomer, R. D. Jones, F. Begay, A. W. Ehier, J. F. Kephart, and R. Kristal, Phys. Fluids **298**, 2679 (1986).
[11] G. Pretzler, A. Saemann, A. Pukhov, D. Rudolph, T. Schatz, U. Schramm, P. Thirolf, D. Habs, K. Eidmann, G. D. Tsakiris, J. Meyer-ter-Vehn, and K. J. Witte, Phys. Rev. E **58**, 1165 (1998).
[12] S. C. Wilks, W. L. Kruer, M. Tabak, and A. B. Langdon, Phys. Rev. Lett. **69**, 1383 (1992).
[13] J. Denavit, Phys. Rev. Lett. **69**, 3052 (1992).
[14] S. C. Wilks, A. B. Langdon, T. E. Cowan, M. Roth, M. Singh, S. Hatchett, M. H. Key, D. Pennington, A. MacKinnon, and R. A. Snavely, Phys. Plasmas **18**, 542 (2001).
[15] L. J. Perkins, B. G. Logan, M. D. Rosen, M. D. Perry, T. Diaz de la Rubia, N. M. Ghoniem, T. Ditmire, P. T. Springer, and S. C. Wilks, Nucl. Fusion **40**, 1 (2000).
[16] M. Borghesi, A. Schiavi, D. H. Campbell, M. G. Haines, O. Willi, A. J. MacKinnon, L. A. Gizzi, M. Galimberti, R. J. Clarke, and H. Ruhl, Plasma Phys. Controlled Fusion **43**, 12A (2001).
[17] M. Borghesi, S. Bulanov, D. H. Campbell, R. J. Clarke, T. Z. Esirkepov, M. Galimberti, L. A. Gizzi, A. J. MacKinnon, N. M. Naumova, F. Pegoraro, H. Ruhl, A. Schiavi, and O. Willi, Phys. Rev. Lett. **88**, 13502 (2002).
[18] M. Borghesi, D. H. Campbell, A. Schiavi, M. G. Haines, O. Willi, A. J. MacKinnon, P. Patel, L. A. Gizzi, M. Galimberti, R. J. Clarke, F. Pegoraro, H. Ruhl, and S. Bulanov, Phys. Plasmas **9**, 2214 (2002).
[19] J. A. Cobble, R. P. Johnson, T. E. Cowan, N. Renard-Le Galloudec, and M. Allen, J. Appl. Phys. **92**, 4 (2002).
[20] A. J. MacKinnon, P. K. Patel, D. W. Price, D. Hicks, M. Borghesi, and L. Romagnani, Rev. Sci. Instrum. **74**, 1917 (2003).
[21] M. Borghesi, A. J. MacKinnon, D. H. Campbell, D. Hicks, S. Kar, D. Price, L. Romagnani, A. Schiavi, and O. Willi, Phys. Rev. Lett. **92**, 05503 (2004).
[22] R. Loveman, J. Bendahan, T. Gozani, and J. Stevenson, Nucl. Instrum. Methods Phys. Res. B **99**, 765 (1995).
[23] G. Chen and R. C. Lancza, IEEE Trans. Nucl. Sci. **49**, 1919 (2002).
[24] J. S. Brzosko, B. V. Robouch, L. Ingrosso, A. Bortolotti, and V. Nardi, Nucl. Instrum. Methods Phys. Res. B **72**, 119 (1992).
[25] L. Disdier, J. P. Garconnet, G. Malka, and J. L. Miquel, Phys. Rev. Lett. **82**, 1454 (1999).
[26] C. N. Danson, J. Collier, D. Neely, L. J. Barzanti, A. Damerell, C. B. Edwards, M. H. R. Hutchinson, M. H. Key, P. A. Norreys, D. A. Pepler, I. N. Ross, P. F. Taday, W. T. Toner, M. Trentelman, F. N. Walsh, T. B. Winstone, and R. W. W. Wyatt, J. Mod. Opt. **45**, 1653 (1997).
[27] J. A. Frenje, C. K. Li, F. H. Ségiun, D. G. Hicks, S. Kurebayashi, R. D. Petrasso, S. Roberts, V. Y. N. Glebov, D. D. Meyerhofer, T. C. Sangster, J. M. Soures, C. Stoeckl, C. Chiritescu, G. J. Schmind, and R. A. Lerche, Rev. Sci. Instrum. **73**, 2597 (2002).
[28] E. L. Clark, K. Krushelnick, M. Zepf, F. N. Beg, M. Tatarakis, A. Machacek, M. I. K. Santala, I. Watts, P. A. Norreys, and A. E. Dangor, Phys. Rev. Lett. **85**, 8 (2000).
[29] S. Karsch, S. Dusterer, H. Schwoerer, F. Ewald, D. Habs, M. Hegelich, G. Pretzler, A. Pukhov, K. Witte, and R. Sauerbrey, Phys. Rev. Lett. **91**, 015001 (2003).
[30] Los Alamos Report LA-12625-M, edited by J. Briesmeister, 1997; http://www-xdiv.lanl.gov/x5/MCNP/index.html.
[31] M. Zepf, E. L. Clark, K. Krushelnick, F. N. Beg, C. Escoda, A. E. Dangor, M. I. K. Santala, M. Tatarakis, I. F. Watts, P. A. Norreys, R. J. Clarke, J. R. Davies, M. A. Sinclair, R. D. Edwards, T. J. Goldsack, I. Spencer, and K. W. D. Ledingham, Phys. Plasmas **8**, 2323 (2001).
[32] M. Matsubayashi, T. Hibiki, K. Mishima, K. Yoshii, K. Okamoto, Nucl. Instrum. Methods Phys. Res. A **463**, 324 (2001).